Arene Ruthenium Complexes Specifically Inducing Apoptosis in Breast Cancer Cells

Adriana Grozav [1,*], Thomas Cheminel [2], Ancuta Jurj [3], Oana Zanoaga [3], Lajos Raduly [3], Cornelia Braicu [3], Ioana Berindan-Neagoe [3], Ovidiu Crisan [1], Luiza Gaina [4,*] and Bruno Therrien [2,*]

[1] Faculty of Pharmacy, "Iuliu Hatieganu" University of Medicine and Pharmacy, Victor Babes 41, 400012 Cluj-Napoca, Romania; ocrisan@umfcluj.ro

[2] Institute of Chemistry, University of Neuchatel, Ave. de Bellevaux 51, 2000 Neuchatel, Switzerland; thomas.cheminel@gbjb.ch

[3] Research Center for Functional Genomics, Biomedicine and Translational Medicine, "Iuliu Hatieganu" University of Medicine and Pharmacy, Marinescu 23, 400337 Cluj-Napoca, Romania; anca.jurj@umfcluj.ro (A.J.); oana.zanoaga@umfcluj.ro (O.Z.); lajos.raduly@umfcluj.ro (L.R.); cornelia.braicu@umfcluj.ro (C.B.); ioana.neagoe@umfcluj.ro (I.B.-N.)

[4] Department of Chemistry, Faculty of Chemistry and Chemical Engineering, Babeş-Bolyai University, 11 Arany Janos Str., 400028 Cluj-Napoca, Romania

* Correspondence: adriana.ignat@umfcluj.ro (A.G.); ioana.gaina@ubbcluj.ro (L.G.); bruno.therrien@unine.ch (B.T.)

Abstract: Monocationic arene ruthenium complexes (**RuL$_1$**–**RuL$_4$**) incorporating phenothiazinyl-hydrazinyl-thiazole ligands (**L$_1$**–**L$_4$**) have been synthesized, characterized and evaluated as anticancer agents. Their cytotoxicity, antiproliferative activity and alteration of apoptotic gene expression were studied on three cancer cell lines, a double positive breast cancer cell line MCF-7 and two triple negative breast cancer cell lines Hs578T and MDA-MB-231. All arene ruthenium complexes were able to reduce the viability of the breast cancer cell lines, with the highest cytotoxicities being recorded for the [(p-cymene)Ru**L$_3$**Cl]$^+$ (**RuL$_3$**) complex on the MCF-7 (IC$_{50}$ = 0.019 μM) and Hs578T cell lines (IC$_{50}$ = 0.095 μM). In the double positive MCF-7 breast cancer cells, the complexes [(p-cymene)Ru**L$_1$**Cl]$^+$ (**RuL$_1$**) and [(p-cymene)Ru**L$_2$**Cl]$^+$ (**RuL$_2$**) significantly upregulated pro-apoptotic genes including BAK, FAS, NAIP, CASP8, TNF, XIAP and BAD, while downregulating TNFSF10. In the triple negative breast cancer cell line Hs578T, **RuL$_1$** reduced TNFSF-10 and significantly upregulated BAK, CASP8, XIAP, FADD and BAD, while complex **RuL$_2$** also increased BAK and CASP8 expression, but had limited effects on other genes. The triple negative MDA-MB-231 cancer cells treated with **RuL$_1$** upregulated NOD1 and downregulated p53, while **RuL$_2$** significantly downregulated p53, XIAP and TNFSF10, with minor changes in other genes. The significant alterations in the expression of key apoptotic genes suggest that such complexes have the potential to target cancer cells.

Keywords: arene ruthenium complexes; phenothiazinyl-hydrazinyl-thiazole ligands; cytotoxicity; apoptosis; gene expression; breast cancer cells; MCF-7; Hs578T; MDA-MB-231

1. Introduction

Human breast cancer, one of the most common types of cancer according to the World Health Organization statistics, has been diagnosed in more than 2.3 million women in 2022 [1]. Triple negative breast cancer (TNBC) is the most aggressive form [2], with patients exhibiting a heightened propensity for early metastasis compared with those with other types of breast cancer [3]. TNBC is defined by a deficiency in progesterone (PR) and estrogen receptors (ER), as well as in human epidermal growth factor receptor 2 (HER2) expression [4,5]. These factors collectively contribute to the TNBC's distinctive biological features, which makes it challenging to treat with current drugs [6–8]. In comparison with TNBC, the double positive breast cancer (ER+/PR+) phenotype is linked to a greater

prevalence among older patients, showing smaller tumors and offering a more favorable prognosis in comparison with the ER+/PR- phenotype [9–11].

Ruthenium complexes are promising chemotherapeutic agents, and several Ru(II) derivatives have entered clinical trials, with, however, variable outcomes [12,13]. Among biologically active Ru(II) complexes, the arene ruthenium family possesses interesting antitumor activity, showing different mechanisms. Some arene ruthenium complexes have the ability to bind DNA in a covalent or non-covalent manner [14,15], while others showed interactions with cytochrome c [16], as well as other biomolecules [17]. Such diversity in their targets and modes of action is linked to their facility to modify their structures and properties by the introduction of a wide range of ligands, thus tuning their cytotoxic effect. For example, against TNBC, arene ruthenium complexes incorporating the bidentate bis(3,5-dimethylpyrazol-1-yl)methane [18] or iminophosphorane ligands [19] showed a suppression of TNBC growth in vivo, while arene ruthenium complexes with α-amino acid ligands (methionine and tryptophan) were able to induce selective apoptosis of MDA-MB-231 cells through DNA interaction [20].

In a previous study, we reported the synthesis and biological activity of hydrazinyl-thiazolo arene ruthenium complexes [21]. All complexes were more active than cisplatin and oxaliplatin on cervical (HeLa) and ovarian (A2780 and A2780cisR) cancer cells [21], and in vivo, the complexes were well tolerated after oral and intraperitoneal administrations in rats without altering the hematological profile [22]. Moreover, considering the antitumor activity of phenothiazinyl-hydrazinyl-thiazole derivatives on hepatic HepG2 and colorectal CC531S cells [23], we decided to extend our investigation on a new family of arene ruthenium complexes (**RuL$_1$–RuL$_4$**) with phenothiazinyl-hydrazinyl-thiazolo ligands (**L$_1$–L$_4$**) and to evaluate their antiproliferative activity against double positive (MCF-7) and triple negative (Hs578T, MDA-MB-231) breast cancer cell lines, as well as non-cancerous breast cells (fR2).

2. Results

The monocationic arene ruthenium complexes (**RuL$_1$–RuL$_4$**) were synthesized by reacting [(*p*-cymene)RuCl$_2$]$_2$ with two equivalents of phenothiazinyl-hydrazinyl-thiazole derivatives (**L$_1$–L$_4$**) in methanol at room temperature (Scheme 1). All complexes were isolated as their chloride salts in good yield, as racemic mixtures. Accordingly, the complexes showed the characteristic diastereotopic protons of the *p*-cymene group in the ^{1}H NMR spectra, which was emphasized by the presence of four doublets between 4 and 5 ppm (aromatic protons of *p*-cymene) and two doublets around 1 ppm (methyl groups of the isopropyl moiety). In addition to the *p*-cymene signals, a triplet and a quadruplet can be associated with the *N*-ethyl group of the phenothiazine moiety at 1.5 and 4.0 ppm, respectively. In the ESI-MS spectra (positive mode), the parent signal is always associated with the cationic complex [(*p*-cymene)RuLCl]$^+$ after the loss of the counteranion.
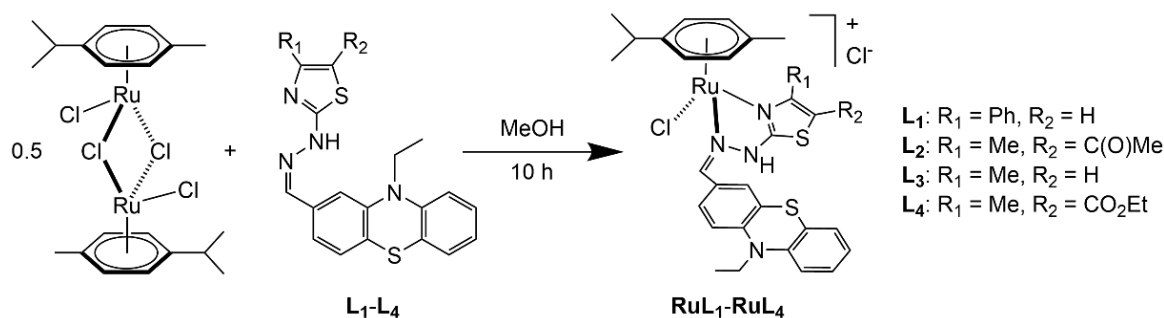
Scheme 1. Synthesis of [(*p*-cymene)RuLCl]Cl (**RuL1–RuL4**) from [(*p*-cymene)RuCl$_2$]$_2$ and the phenothiazinyl-hydrazinyl-thiazole ligands (**L1–L4**).

Then, the antiproliferative activity of all complexes was determined on various cell lines using MTT assays, the NBC cell lines (MDA-MB-231, Hs578T and MCF-7) as well as the

non-cancerous breast cells (fR2). The complexes were initially dissolved in DMSO, and stock solutions of 1.0 M concentration were used to prepare biological solutions (concentrations ranging from 10 nM to 10^4 nM) for the in vitro tests, thus never exceeding 1% of DMSO. The stability of the complexes under physiological conditions was not studied in detail, however, aquation cannot be excluded [24], and the chelating ligand (**L**) is more strongly coordinated than the chloride, thus ensuring that the active complexes have an arene ruthenium phenothiazinyl-hydrazinyl-thiazolo structure. All cell lines were incubated for 24 h with the complexes **RuL1–RuL4**. The MTT values after 24 h incubation expressed as % of control according to the log(concentration, nM) were determined (Figure 1). The IC_{50} values for each compound are presented in Table 1.
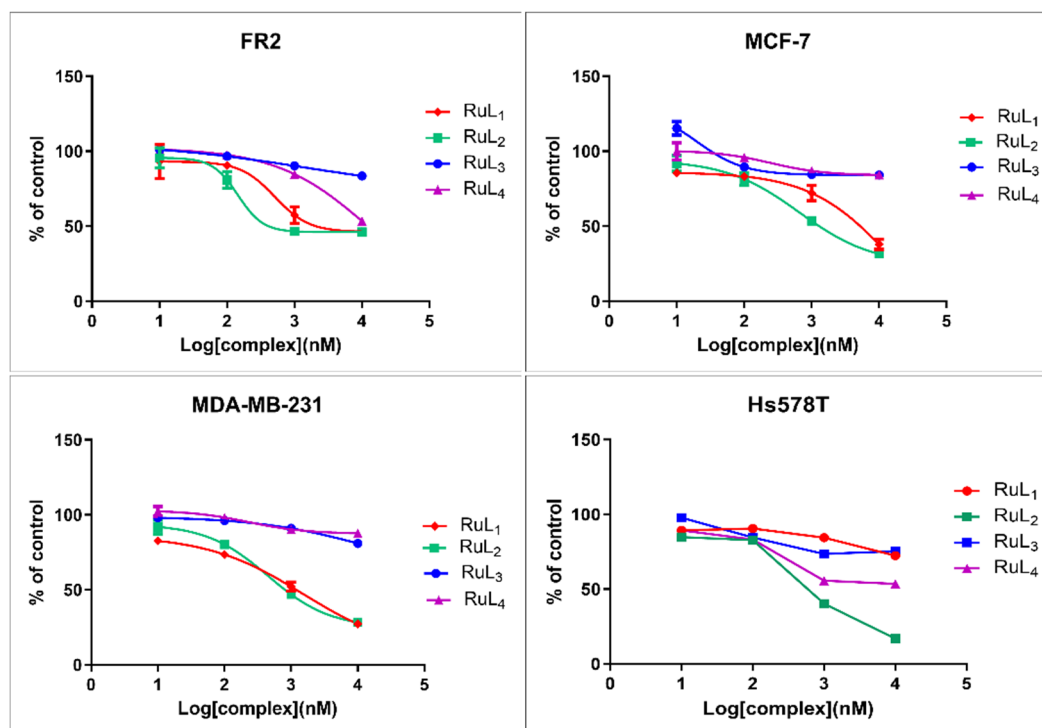
Figure 1. Antiproliferative effects determined from MTT assays after 24 h incubation with **RuL1–RuL4** on NBC cells (MCF-7, MDA-MS-231, Hs578T) and normal cells (fR2). Log(conc, nM) = Log(concentration of complexes, nM) (mean $\pm$ SD, n = 6).

The MTT assays show that all complexes reduced the viability of breast cancer cell lines after 24 h of incubation at low µM concentrations. For the MCF-7 and MDA-MB-231 cancer cell lines, complexes **RuL1** and **RuL2** showed cell viability below 35% compared with the control experiment (cells incubated in the absence of complexes), while for the Hs578T cell lines, only **RuL2** reduced cell viability below 15%, with the other complexes having a lower inhibitory activity. Based on these MTT assays, the IC_{50} values for each complex were determined (Table 1).

The lowest IC_{50} value was recorded for **RuL3** (0.019 µM) on the double positive breast cancer cell line MCF-7, followed by the same complex on the triple negative breast cancer cell line Hs578T (0.095 µM). This complex showed the highest cytotoxicity among all complexes investigated but remained less cytotoxic on the triple negative breast cancer cell line MDA-MB-231 (14.125 µM). On the other hand, **RuL2** showed a high degree of cytotoxicity on all cancer cell lines, MCF-7 (0.654 µM), MDA-MB-231 (0.449 µM) and Hs578T (0.705 µM), compared with **RuL1**, but was less cytotoxic than **RuL3** on the MCF-7 and Hs578T breast tumor cell lines. Overall, for complexes **RuL1** and **RuL2**, the IC_{50} values were much more homogenous and showed a superior correlation coefficient (R^2), thus encouraging us to select **RuL1** and **RuL2** for further investigations.

Table 1. IC$_{50}$ values of **RuL1–RuL4** determined from the MTT assays.

Cell Line Name	Compound	IC$_{50}$ [μM]
MDA-MB-231	**RuL$_1$**	1.496
	RuL$_2$	0.449
	RuL$_3$	14.125
	RuL$_4$	0.229
Hs578T	**RuL$_1$**	1.186
	RuL$_2$	0.705
	RuL$_3$	0.095
	RuL$_4$	0.228
MCF-7	**RuL$_1$**	14.514
	RuL$_2$	0.654
	RuL$_3$	0.019
	RuL$_4$	0.247
fR2	**RuL$_1$**	0.51
	RuL$_2$	0.144
	RuL$_3$	1.26
	RuL$_4$	12.55

The MTT results showed a decrease in cell proliferation, which could be associated with an increase in the number of apoptotic cells. Therefore, we evaluated the apoptosis rate of normal and breast cancer cell lines exposed to **RuL$_1$** and **RuL$_2$**, at their respective IC$_{50}$ concentrations (Figure 2). Twenty-four hours after treatment, cell death was assessed via fluorescence microscopy after staining with DAPI (4′,6-diamidino-2-phenylindole), a dye that specifically stains cell nuclei. As shown in Figure 2A, DAPI staining of the control group displayed intact and round nuclei, indicating that cells were not undergoing apoptosis. In treated cells, the number of viable cells decreased and fragmented nuclei were observed. In addition, both compounds exhibited visible pro-apoptotic effects on breast cell lines at 24 h post-treatment. Interestingly, **RuL$_2$** showed a higher percentage of apoptotic cells than **RuL$_1$** (Figure 2B), with the most pronounced effect observed in fR2 cells for **RuL$_2$**, being in agreement with the MTT data.

We also evaluated the mode of action of **RuL$_1$** and **RuL$_2$** at the IC$_{50}$ concentrations. Based on the MTT and apoptosis results, we selected for the qRT-PCR (real-time quantitative reverse transcription PCR) genes, which were strongly involved in apoptotic processes including TNFSF10 (Tumor Necrosis Factor Superfamily Member 10), NOD1 (Nucleotide Binding Oligomerization Domain Containing 1), CASP8 (Caspase 8), FADD (Fas Associated via Death Domain), NAIP (NLR Family Apoptosis Inhibitory Protein), FAS (Fas Cell Surface Death Receptor), BAD (BCL2 Associated Agonist of Cell Death), p53 (tumor protein p53), TNF (Tumor Necrosis Factor), BAK1 (BCL2-antagonist/killer 1) and XIAP (X-Linked Inhibitor of Apoptosis).

In the normal cell line fR2, treatment with **RuL$_1$** and **RuL$_2$** led to specific changes in apoptotic gene expression, with **RuL$_1$** causing downregulation of CASP8 and p53, while **RuL$_2$** upregulated BAK; however, changes in NAIP, FAS, FADD and TNFSF10 were not statistically significant. In double positive MCF-7 cells, both complexes significantly increased the levels of pro-apoptotic genes including BAK, FAS, NAIP, CASP8, TNF, XIAP and BAD, although changes in p53, FADD and NOD1 lacked statistical significance, and TNFSF10 expression decreased without statistical relevance. For triple negative Hs578T cells, **RuL$_1$** reduced TNFSF10 expression and enhanced levels of BAK, CASP8, XIAP, FADD, BAD and TNF, while **RuL$_2$** similarly increased BAK, NAIP, CASP8 and TNF but caused only

a slight and non-significant decrease in FAS expression. In triple negative MDA-MB-231 cells, **RuL₁** treatment resulted in increased NOD1 and decreased p53 expression, with other genes showing non-significant changes, whereas **RuL₂** significantly lowered p53, XIAP and TNFSF10 levels, with slight upregulation of BAK and non-significant alterations in NAIP, TNF, FADD and BAD.
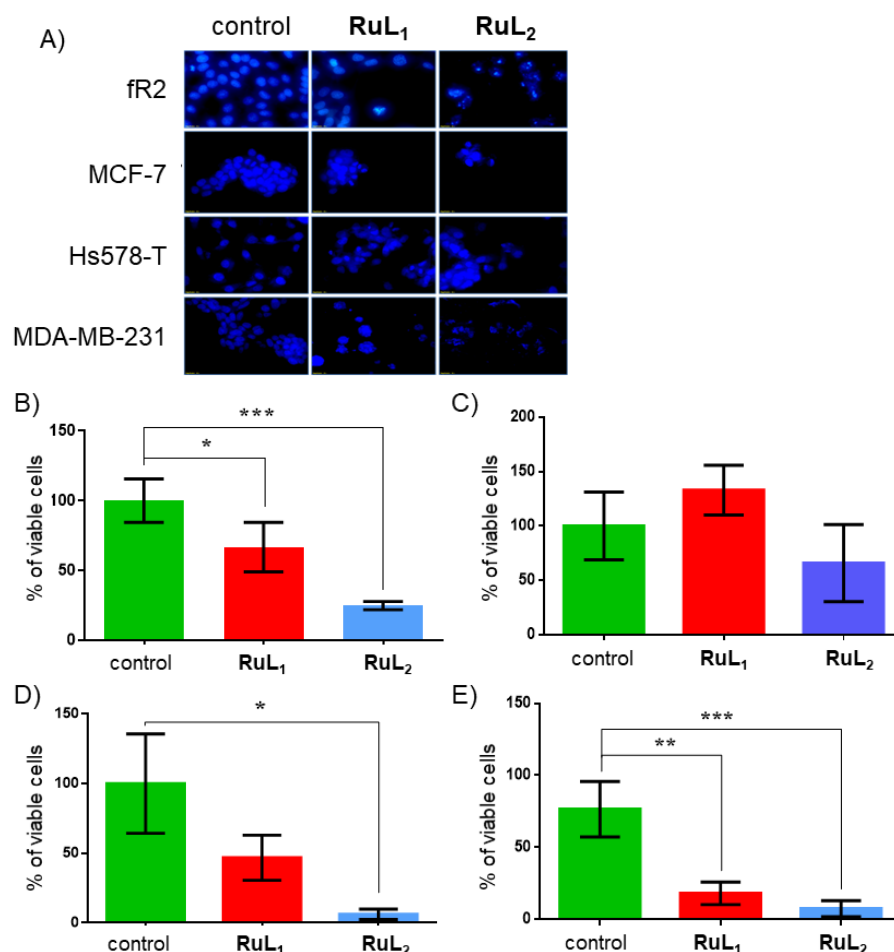
Figure 2. (**A**) Fluorescence microscopy, showing nuclear features after DAPI staining on normal and NBC cell lines after 24 h incubation (40x magnification). Statistical analysis on various cell lines. (**B**) Normal cell line fR2. (**C**) Triple negative breast cancer cell line, Hs578T. (**D**) Double positive breast cancer cell line (data presented as mean ± SD; p * = 0.039 for compound 2, two-side *t*-test). (**E**) Triple negative breast cancer cell line, MDA-MB-231 (data presented as mean ± SD; p ** = 0.0047 for **RuL₁**, p *** = 0.0001 for **RuL₂**, two-side *t*-test).

In the case of the triple negative breast cancer cell line Hs578T, we observed that **RuL₁** inhibited the relative gene expression of TNFSF10 in comparison with the control group. In addition, the expression levels of BAK1, CASP8, XIAP, FADD, BAD and TNF were statistically overexpressed compared with the control group. In the case of the FAS gene, the expression level was slightly decreased but not statistically significant. Otherwise, gene expression profiling in **RuL₂** was statistically overexpressed compared with control (Table 2, Figure 3). The second triple negative breast cancer cell line, MDA-MB-231, treated with **RuL₁,** did not alter the expression levels of the selected genes. The NOD1 gene exhibited a statistically upregulated level, while the p53 gene exhibited a statistically downregulated level compared with the control group. BAK and TNF genes showed an increased expression level and XIAP, FADD, TNFSF10 and BAD and a decreased profiling with no significant p values. **RuL₂** statistically decreased significantly the expression of p53, XIAP and TNFSF10. However, **RuL₂** slightly upregulated the BAK1 level and respectively

decreased the NAIP, TNF, FADD and BAD levels, with no significant *p* values compared with the control group (Table 2, Figure 3).

Table 2. Gene expression assessments, as an effect of **RuL₁** and **RuL₂** treatment on breast cell lines (cut-off value of expression fold change FC $\pm$ 1.25 and *p*-value ≤ 0.05).

Cell Line	Compound	Gene	FC	*p*-Value
fR2	**RuL₁**	CASP8	−2.36	0.0032
		p53	−1.72	0.0025
		TNFSF10	−2.21	0.0043
	RuL₂	BAK	1.48	0.048
		CASP8	−1.84	5.12
		p53	−1.35	0.0080
MCF-7	**RuL₁**	BAK	4.04	0.019
		FAS	3.43	0.0091
		NAIP	2.27	0.0013
		CASP8	4.51	0.0099
		TNF	18.51	0.0036
		XIAP	2.11	0.011
		BAD	2.27	0.021
	RuL₂	BAK	4.04	0.011
		FAS	20.28	0.0043
		NAIP	3.98	0.0057
		CASP8	2.4	0.0069
		TNF	24.93	0.0069
		p53	1.56	0.16
		XIAP	2.13	0.0019
		FADD	1.91	0.10
		BAD	7.22	0.0044
Hs578T	**RuL₁**	BAK	3.09	0.0044
		CASP8	2.02	0.019
		TNF	2.12	1.77
		XIAP	1.65	0.0056
		FADD	2.41	0.0091
		BAD	2.24	0.027
		TNFSF10	−5.5	0.035
	RuL₂	BAK	5.79	8.86
		NAIP	3.15	0.022
		CASP8	3.37	0.0011
		TNF	12.36	0.00011
		p53	1.89	0.0034
		NOD1	2.31	0.0060
		XIAP	4.44	3.61
		FADD	5.34	0.0015
		BAD	2.92	0.0068

Table 2. *Cont.*

Cell Line	Compound	Gene	FC	*p*-Value
MDA-MB-231	RuL$_1$	NOD1	1.44	0.030
		p53	−2.09	0.0021
	RuL$_2$	p53	−1.58	0.0056
		XIAP	−1.72	0.0047
		TNFSF10	−2.32	0.014
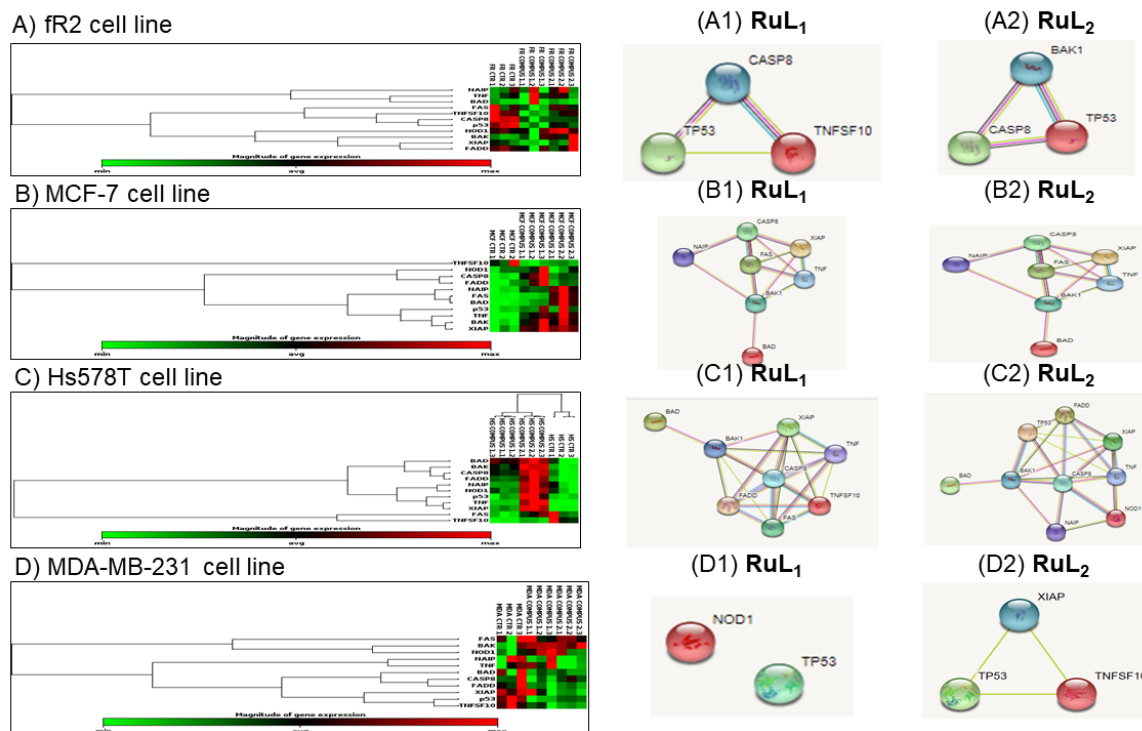
Figure 3. Expression profile of selected genes in normal and breast cancer cell lines after incubation with **RuL$_1$** and **RuL$_2$** for 24 h. (**A–D**) The heatmap presents genes for breast cancer cell lines (color bars represent gene expression fold change: red color indicates the increased level and green indicates the decreased expression level in treated cells); (**A1,B1,C1,D1**) represents the STRING network [25] for the genes with an altered expression level for genes of at least 1.25-fold increase or decrease with a *p*-value ≤ 0.05 as effect of **RuL$_1$** treatment; (**A2,B2,C2,D2**) represents the STRING network for the genes with an altered expression level considering the same cut-off values effect of the **RuL$_2$** treatment.

3. Discussion

Ruthenium complexes trigger cell-specific responses with variable toxicity and subsequent cell fate depending on the type of breast cancer cells. The ruthenium complexes, in particular **RuL$_3$** and **RuL$_2$**, showed potent cytotoxic effects against various breast cancer cell lines, with **RuL$_3$** showing the highest cytotoxicity in both MCF-7 and Hs578T cells. The mechanism of action involves the induction of apoptosis, with variations in apoptotic gene expression profiles across the cell lines. This highlights the complex nature of ruthenium interactions with cancer cells.

The treatment of breast cancer cell lines with ruthenium complexes **RuL$_1$** and **RuL$_2$** resulted in significant alterations in the expression of key apoptotic genes, reflecting their potential as therapeutic agents. In normal fR2 cells, **RuL$_1$** and **RuL$_2$** predominantly affected CASP8 and p53, while **RuL$_2$** also upregulated BAK. In the MCF-7 breast carcinoma cell line, both complexes notably increased the expression of pro-apoptotic genes such as BAK, FAS, NAIP, CASP8, TNF, XIAP and BAD, while reducing TNFSF10 levels. Similarly, in the

triple negative breast cancer cell line Hs578T, **RuL$_1$** decreased TNFSF10 and significantly upregulated BAK, CASP8, XIAP, FADD and BAD, while **RuL$_2$** also enhanced BAK and CASP8 expression but had variable effects on the other genes. MDA-MB-231 cells treated with **RuL$_1$** showed upregulation of NOD1 and downregulation of p53, while **RuL$_2$** led to significant decreases in p53, XIAP and TNFSF10, with minor changes in other genes. These findings highlight the ability of ruthenium complexes incorporating phenothiazinyl-hydrazinyl-thiazolo ligands to modulate apoptotic pathways in a cell type-specific manner, confirming their potential utility in targeted cancer therapy.

4. Materials and Methods

All chemicals, reagents and solvents were purchased from commercial suppliers and used without further purification unless otherwise stated. The ^{1}H NMR spectra were recorded in solution (CDCl$_3$) at room temperature on a Bruker Avance II 400 spectrometer, using an internal standard. Elemental analyses were performed by the Mikroelementarisches Laboratorium, ETH Zürich. Mass spectra (electrospray ionization, positive-ion mode) were recorded with a Bruker FTMS 4.7T BioAPEX II mass spectrometer. The phenothiazinyl-hydrazinyl-thiazole derivatives (**L1**–**L4**) were prepared according to published method [23].

4.1. Synthesis and Characterization of Compounds RuL$_1$–RuL$_4$

The dinuclear complex [(*p*-cymene)RuCl$_2$]$_2$ (100 mg; 0.163 mmol) and the corresponding **L$_1$**–**L$_4$** phenothiazinyl-hydrazinyl-thiazole (0.327 mmol) were dissolved in methanol (50 mL) and stirred at room temperature for 10 h. Then, the solvent was removed under vacuum. The residue was dissolved in dichloromethane (5 mL), and 200 mL of *n*-hexane was added to initiate the precipitation of the salts. The precipitate was filtered, washed several times with *n*-hexane, and dried under vacuum to give the corresponding product in good yield.

RuL$_1$: [(*p*-cymene)Ru**L$_1$**Cl]Cl, yellow-green powder, yield 75%. ^{1}H NMR (CDCl$_3$, 400 MHz): δ = 1.02 (d, $^3J_{\text{H-H}}$ = 6.6 Hz, 3H), 1.07 (d, $^3J_{\text{H-H}}$ = 6.6 Hz, 3H), 1.52 (t, $^3J_{\text{H-H}}$ = 7.0 Hz, 3H), 2.25 (s, 3H), 2.50 (sept, $^3J_{\text{H-H}}$ = 6.6 Hz, 1H), 4.03 (q, $^3J_{\text{H-H}}$ = 7.0 Hz, 2H), 4.05 (d, $^3J_{\text{H-H}}$ = 5.7 Hz, 1H), 4.75 (d, $^3J_{\text{H-H}}$ = 5.7 Hz, 1H), 4.82 (d, $^3J_{\text{H-H}}$ = 5.7 Hz, 1H), 4.86 (d, $^3J_{\text{H-H}}$ = 5.7 Hz, 1H), 6.76 (s, 1H), 6.98–7.01 (m, 3H), 7.20–7.22 (m, 2H), 7.58–7.60 (m, 3H), 7.83 (m, 1H), 7.97–7.98 (m, 2H), 8.32 (s, 1H), 9.14 (s, 1H), 15.35 (s, 1H) ppm. IR (KBr pellet): 2918 (m), 1575 (m), 1466 (s), 1384 (m), 1243 (m), 1053 (w), 752 (w) cm^{-1}. ESI-MS *m/z* (+): 699.1 [M-Cl]$^+$. Anal. Calcd for C$_{34}$H$_{34}$N$_4$S$_2$Cl$_2$Ru: C, 55.65; H, 4.53; N, 7.64; S, 8.74. Found: C, 55.23; H, 4.33; N, 7.56; S, 8.64.

RuL$_2$: [(*p*-cymene)Ru**L$_2$**Cl]Cl, yellow-orange powder, yield 77%. ^{1}H NMR (CDCl$_3$, 400 MHz): δ = 1.12 (d, $^3J_{\text{H-H}}$ = 6.7 Hz, 3H), 1.21 (d, $^3J_{\text{H-H}}$ = 6.7 Hz, 3H), 1.52 (t, $^3J_{\text{H-H}}$ = 6.8 Hz, 3H), 2.35 (s, 3H), 2.46 (s, 3H), 2.86 (s, 3H), 3.18 (sept, $^3J_{\text{H-H}}$ = 6.7 Hz, 1H), 4.03 (q, $^3J_{\text{H-H}}$ = 6.8 Hz, 2H), 4.94 (d, $^3J_{\text{H-H}}$ = 5.9 Hz, 1H), 5.27 (d, $^3J_{\text{H-H}}$ = 5.9 Hz, 1H), 5.47 (d, $^3J_{\text{H-H}}$ = 5.9 Hz, 1H), 5.58 (d, $^3J_{\text{H-H}}$ = 5.9 Hz, 1H), 6.97–6.98 (m, 4H), 7.18–7.19 (m, 2H), 8.25 (s, 1H), 9.06 (s, 1H) ppm, 15.23 (s, 1H) ppm. IR (KBr pellet): 2921 (m), 1624 (s), 1468 (s), 1245 (m), 1110 (m), 751 (m) cm^{-1}. ESI-MS *m/z* (+): 679.1 [M-Cl]$^+$. Anal. Calcd for C$_{31}$H$_{34}$N$_4$OS$_2$Cl$_2$Ru: C, 52.17; H, 4.66; N, 7.85; S, 8.99. Found: C, 52.12; H, 4.58; N, 7.71; S, 8.89.

RuL$_3$: [(*p*-cymene)Ru**L$_3$**Cl]Cl, yellow-green powder, yield 68%. ^{1}H NMR (CDCl$_3$, 400 MHz): δ = 1.08 (d, $^3J_{\text{H-H}}$ = 6.5 Hz, 3H), 1.18 (d, $^3J_{\text{H-H}}$ = 6.5 Hz, 3H), 1.48 (t, $^3J_{\text{H-H}}$ = 6.7 Hz, 3H), 2.34 (s, 3H), 2.46 (s, 3H), 2.65 (sept, $^3J_{\text{H-H}}$ = 6.5 Hz, 1H), 3.99 (q, $^3J_{\text{H-H}}$ = 6.7 Hz, 2H), 4.93 (d, $^3J_{\text{H-H}}$ = 5.6 Hz, 1H), 5.22 (m, 2H), 5.47 (d, $^3J_{\text{H-H}}$ = 5.6 Hz, 1H), 6.46 (s, 1H), 6.95–6.96 (m, 4H), 7.16–7.17 (m, 2H), 8.25 (s, 1H), 9.11 (s, 1H), 15.02 (s, 1H) ppm. IR (KBr pellet): 2921 (m), 1623 (s), 1466 (s), 1242 (m), 1136 (m), 753 (m) cm^{-1}. ESI-MS *m/z* (+): 637.1 [M-Cl]$^+$. Anal. Calcd for C$_{29}$H$_{32}$N$_4$S$_2$Cl$_2$Ru: C, 51.86; H, 4.65; N, 8.34; S, 9.55. Found: C, 51.77; H, 4.57; N, 8.24; S, 9.43.

RuL$_4$: [(*p*-cymene)RuL$_4$Cl]Cl, yellow-orange powder, yield 82%. ^{1}H NMR (CDCl$_3$, 400 MHz): δ = 1.09 (d, $^3J_{\text{H-H}}$ = 6.7 Hz, 3H), 1.18 (d, $^3J_{\text{H-H}}$ = 6.7 Hz, 3H), 1.33 (t, $^3J_{\text{H-H}}$ = 7.1 Hz, 3H), 1.49 (t, $^3J_{\text{H-H}}$ = 6.9 Hz, 3H), 2.37 (s, 3H), 2.62 (sept, $^3J_{\text{H-H}}$ = 6.7 Hz, 1H), 2.82 (s, 3H), 4.00 (q, $^3J_{\text{H-H}}$ = 6.9 Hz, 2H), 4.30 (q, $^3J_{\text{H-H}}$ = 7.1 Hz, 2H), 4.93 (d, $^3J_{\text{H-H}}$ = 5.6 Hz, 1H), 5.24 (m, 2H), 5.47 (d, $^3J_{\text{H-H}}$ = 5.6 Hz, 1H), 6.96–6.97 (m, 4H), 7.14–7.15 (m, 2H), 8.25 (s, 1H), 9.08 (s, 1H), 15.92 (s, 1H) ppm. IR (KBr pellet): 2969 (m), 1599 (s), 1465 (s), 1372 (m), 1271 (m), 1098 (s), 753 (m) cm^{-1}. ESI-MS *m/z* (+): 709.1 [M-Cl]$^+$. Anal. Calcd for C$_{32}$H$_{36}$N$_4$O$_2$S$_2$Cl$_2$Ru: C, 51.68; H, 4.74; N, 7.53; S, 8.62. Found: C, 50.05; H, 4.68; N, 7.41; S, 8.55.

4.2. Cell Lines and Cell Culture

Two human triple negative breast cancer cell lines, MDA-MB-231 and Hs578T, a double positive breast cancer cell line, MCF-7, and a normal breast cell line, fR2, were purchased from the American Type Culture Collection (ATCC). MDA-MB-231 cells were cultured in RPMI-1640 medium (Gibco) supplemented with 10% fetal bovine serum (FBS, Gibco) and 1% penicillin-streptomycin (Gibco). The Hs578T cell line was maintained in D-MEM high glucose supplemented (Gibco) with 10% FBS, 1% penicillin-streptomycin, 2 mM L-glutamine (Gibco), 0.01 mg/mL insulin, 1% MEM-NEEA (MEM Non-Essential Amino Acids Solution, Gibco) and 1% penicillin-streptomycin. The MCF-7 cell line was cultured in MEM (Minimum Essential Medium Eagle, Gibco) supplemented with 10% FBS, 2 mM L-glutamine, 1% MEM-NEEA and 1% penicillin-streptomycin. Normal breast cells, fR2, were cultured in RPMI-1640, 10% FBS, 0.01 mg/mL insulin and 1% penicillin-streptomycin. The cells were grown in a humidified atmosphere at 37 °C with 5% CO$_2$.

4.3. Cell Viability Assay

Cell viability was assessed by the MTT assay (MTT = 3-(4,5-dimethylthiazol-2-yl)-2,5-diphenyl-2H-tetrazolium bromide) in accordance with the manufacturer's protocol. At a seeding density of 10^4 cells/well, cells were seeded in a 96-well plate and incubated at 37 °C with 5% CO$_2$. Twenty-four hours after incubation, the cells were treated with the appropriate therapeutic dose of the **RuL$_1$**–**RuL$_4$** and incubated for 24 h. The complexes were initially dissolved in DMSO, and stock solutions of 1.0 M concentration were used to prepare the biological solutions (concentrations ranging from 10 nM to 10^4 nM). To evaluate the proliferative activity of the cells, 1 mg/mL MTT solution was added and incubated for 1 h. The formazan obtained after intracellular reduction of 3-(4,5-dimethylthiazol-2-yl)-2,5-diphenyltetrazolium bromide was spectrophotometrically quantified by dissolving formazan in dimethyl sulfoxide and measuring the absorbance after 15 min using a plate reader at a wavelength of 570 nm.

4.4. DAPI Staining

Nucleus traits were assessed using DAPI staining, 10^4 cells/well were seeded and treated with **RuL$_1$** or **RuL$_2$** 24 h later, and after incubation, DAPI solution was added to each well and incubated for a further 5 min at 37 °C. After rinsing with 1X PBS, fluorescence microscopy was used to visualize nucleus features.

4.5. RNA Extraction, cDNA Synthesis and RT-PCR

Cells (seeding density of 5×10^5 cells/well) were treated with the appropriate IC$_{50}$ doses of **RuL$_1$**–**RuL$_4$**, determined for each cell line, and incubated for 24 h. Total RNA was extracted from all cell lines using TriReagent (Invitrogen) in agreement with the producer's procedure. RNA concentration and quality were assessed using a Nanodop-1000 spectrophotometer (Thermo Scientific, Waltham, MA, USA). The amount of 1000 ng of total RNA was reversed transcribed into cDNA using a Transcriptor First Strand cDNA Synthesis Kit (Roche, Basel, Switzerland) based on the producer's guidelines.

The gene expression evaluation was conducted using a TaqMan Fast Advanced Master Mix (Applied Biosystems, Waltham, MA, USA) based on the producer's guidelines and

qRT-PCR was performed on a ViiA7 System (Applied Biosystems). Each sample was analyzed in duplicate in a 10 μL volume using a 384-well plate.

The internal standard controls used were 18S and GAPDH rRNA, and the genes evaluated were BAK, FAS, NAIP, CASP8, TNF, p53, NOD1, XIAP, FACC, TNFSF10 and BAD. Data analysis was performed using the Qiagen online tool based on the ΔΔCt method. (https://www.qiagen.com/us/service-and-support/learning-hub/technologies-and-research-topics/rna-universe/gene-expression/data-analysis/, accessed on 1 November 2022).

TNFSF10: right CAGAGCCTTTTCATTCTTGGA: left CCTCAGAGAGTAGCAGCT-CACA

NOD1: right GGCGAGATACTTCCCTCCTT: left GAATGCAAAGGCCTCACG

CASP8: right TTTCTGCTGAAGTCCATCTTTTT: left TAGGGGACTCGGAGACTGC

FADD: right AGGTCTAGGCGCTCTGC: left CCGAGCTCAAGTTCCTATGC

NAIP: right TGGGAGAATCCTCTCGTCAGA: left CTGGCCAGCATTCTCCTCTA

FAS: right GAGACGAAGCTCACGAAAAGC: left GGCCAAGTTGCTGAATCAAT

BAD: right GCTTCCTCTCCCACCGTAG: left ACCCGGAGACAGATGAG

p53: left TCAACAAGATGTTTTGCCAACTG: right TGTGCTGTGACTGCTTGTA-GATG

TNF right GGGGAACTCTTCCCTCTG: left CAGCCTCTTCTCCTTCCTGAT

BAK1: right CCGCGAGACTCCAGTGAT: left GGCCCACAGAGCAACTTCC

GAPDH: right CACCTTCCCCATGGTGTCT: left CCCCGGTTTCTATAAATTGAGC

18S: right CGCTCCACCAACTAAGAACG: left CTCAACACGGGAAACCTCAC

4.6. Statistical Analysis

Results are reported as mean ± SD (standard deviation). The differences between the analyzed **RuL₁**–**RuL₄** activity on cancer cells and controls were analyzed using the *t*-test ($p \leq 0.005$ was considered statistically significant). Statistical analyses were performed using GraphPad Prism version 6 software [26] and STRING 8.0 free version [25].

5. Conclusions

Four new monocationic arene Ru(II) complexes with bidentate phenothiazinyl-hydrazinyl-thiazolo ligands were prepared and their cytotoxicity, antiproliferative activity and alteration of apoptotic gene expression were investigated on three cancer cell lines, a double positive breast cancer cell line, MCF-7, and two triple negative breast cancer cell lines, Hs578T and MDA-MB-231. Two complexes, **RuL₁** and **RuL₂**, have shown significant alterations in the expression of key apoptotic genes, highlighting the ability of such complexes to modulate apoptotic pathways in a cell type-specific manner, thus confirming their potential as anticancer agents. Future research should focus on elucidating the detailed mechanisms of cellular internalization in view of generating ruthenium complexes with enhanced selectivity and efficacy toward tumor cells, while minimizing off-target effects on normal cells.

Author Contributions: Conceptualization, A.G. and C.B.; methodology, A.G. and B.T.; validation, I.B.-N., L.G. and A.G.; formal analysis, O.C., T.C., A.G. and C.B; investigation, A.G., T.C., A.J., L.R. and O.Z.; resources, B.T., I.B.-N. and L.G.; data curation, B.T.; writing—original draft preparation, B.T., L.G.; writing—review and editing, B.T.; supervision, B.T. and A.G.; project administration, B.T. and A.G.; funding acquisition, B.T. All authors have read and agreed to the published version of the manuscript.

Data Availability Statement: The raw data supporting the conclusions of this article will be made available by the authors on request.

Conflicts of Interest: The authors declare no conflicts of interest.

References

1. De Cicco, P.; Catani, M.V.; Gasperi, V.; Sibilano, M.; Quaglietta, M.; Savini, I. Nutrition and Breast Cancer: A Literature Review on Prevention, Treatment and Recurrence. *Nutrients* **2019**, *11*, 1514. [CrossRef] [PubMed]
2. Yang, F.-W.; Mai, T.-L.; Lin, Y.-C.J.; Chen, Y.-C.; Kuo, S.-C.; Lin, C.-M.; Lee, M.-H.; Su, J.-C. Multipathway regulation induced by 4-(phenylsulfonyl)morpholine derivatives against triple-negative breast cancer. *Arch. Pharm. Chem. Life Sci.* **2024**, *357*, 2300435. [CrossRef] [PubMed]
3. Ciocan-Cartita, C.A.; Jurj, A.; Zanoaga, O.; Cojocneanu, R.; Pop, L.; Moldovan, A.; Moldovan, C.; Zimta, A.A.; Raduly, L.; Pop-Bica, C.; et al. New insights in gene expression alteration as effect of doxorubicin drug resistance in triple negative breast cancer cells. *J. Exp. Clin Cancer Res.* **2020**, *39*, 241. [CrossRef] [PubMed]
4. Park, S.-Y.; Choi, J.-H.; Nam, J.-S. Targeting Cancer Stem Cells in Triple-Negative Breast Cancer. *Cancers* **2019**, *11*, 965. [CrossRef]
5. Keskinkılıc, M.; Gökmen-polar, Y.; Badve, S.S. Triple Negative Breast Cancers: An Obsolete Entity ? *Clin. Breast Cancer* **2024**, *24*, 1–6. [CrossRef]
6. Braicu, C.; Pileczki, V.; Pop, L.; Petric, R.C.; Chira, S.; Pointiere, E.; Achimas-Cadariu, P.; Berindan-Neagoe, I. Dual Targeted Therapy with p53 siRNA and Epigallocatechingallate in a Triple Negative Breast Cancer Cell Model. *PLoS ONE* **2015**, *10*, e0120936. [CrossRef]
7. Braicu, C.; Chiorean, R.; Irimie, A.; Chira, S.; Tomuleasa, C.; Neagoe, E.; Paradiso, A.; Achimas-Cadariu, P.; Lazar, V.; Berindan-Neagoe, I. Novel insight into triple-negative breast cancers, the emerging role of angiogenesis, and antiangiogenic therapy. *Expert Rev. Mol. Med.* **2016**, *18*, e18. [CrossRef]
8. Pop, L.; Braicu, C.; Budisan, L.; Morar, G.B.; Monroig-Bosque, P.C. Double gene siRNA knockdown of mutant p53 and TNF induces apoptosis in triple-negative breast cancer cells. *OncoTargets Ther.* **2016**, *9*, 6921–6933. [CrossRef]
9. Ng, C.; Pathy, N.B.; Taib, N.A.; Ho, G.; Mun, S.; Rhodes, A.; Looi, L.-M.; Yip, C.-H. Do Clinical Features and Survival of Single Hormone Receptor Positive Breast Cancers Differ from Double Hormone Receptor Positive Breast Cancers ? *Asian Pac. J. Cancer Prev.* **2014**, *15*, 7959–7964. [CrossRef]
10. Gamrani, S.; Boukansa, S.; Benbrahim, Z.; Mellas, N.; Alaoui, F.F.; Melhouf, M.A.; Bouchikhi, C.; Banani, A.; Boubbou, M.; Bouhafa, T.; et al. The Prognosis and Predictive Value of Estrogen Negative/Progesterone Positive (ER−/PR+) Phenotype: Experience of 1159 Primary Breast Cancer from a Single Institute. *Breast J.* **2022**, *2022*, 9238804. [CrossRef]
11. Wei, S. Hormone receptors in breast cancer: An update on the uncommon subtypes. *Pathol. Res. Pract.* **2023**, *250*, 154791. [CrossRef] [PubMed]
12. Kannan, N.; Radhakrishnan, V.; Sinha, A. Unveiling the anticancer activity of ruthenium and iron complexes. *Inorg. Chem. Commun.* **2024**, *165*, 112512. [CrossRef]
13. Swaminathan, S.; Haribabu, J.; Kavembu, R. From concept to Cure: The Road Ahead for Ruthenium-Based Anticancer Drugs. *ChemMedChem* **2024**, e202400435. [CrossRef] [PubMed]
14. Ganeshpandian, M.; Loganathan, R.; Suresh, E.; Riyasdeen, A.; Akbarsha, M.A.; Palaniandavar, M. New ruthenium(II) arene complexes of anthracenyl-appended diazacycloalkanes: Effect of ligand intercalation and hydrophobicity on DNA and protein binding and cleavage and cytotoxicity. *Dalton Trans.* **2014**, *43*, 1203–1219. [CrossRef]
15. Kasim, M.; Subarkhan, M.; Ramesh, R. Ruthenium(II) arene complexes containing benzhydrazone ligands: Synthesis, structure and antiproliferative activity. *Inorg. Chem. Front.* **2016**, *3*, 1245–1255. [CrossRef]
16. Biancalana, L.; Pratesi, A.; Chiellini, F.; Zacchini, S.; Funaioli, T.; Gabbiani, C.; Marchetti, F. Ruthenium Arene Complexes with Triphenylphosphane Ligands: Cytotoxic Activity Towards Pancreatic Cancer Cells, Interaction with Model Proteins, and Critical Effect of Ethacrynic Acid Substitution. *New J. Chem.* **2017**, *41*, 14574–14588. [CrossRef]
17. Mannancherril, V.; Therrien, B. Strategies toward the enhanced permeability and retention effect by increasing the molecular weight of arene ruthenium metallaassemblies. *Inorg. Chem.* **2018**, *57*, 3626–3633. [CrossRef]
18. Montani, M.; Badillo, G.V.; Hysi, A.; Lupidi, G.; Pettinari, R.; Gambini, V.; Tilio, M.; Marchetti, F.; Pettinari, C.; Ferraro, S.; et al. The water soluble ruthenium(II) organometallic compound [Ru(*p*-cymene)(bis(3,5-dimethylpyrazol-1-yl)methane)Cl]Cl suppresses triple negative breast cancer growth by inhibiting tumor infiltration of regulatory T cells. *Pharmacol. Res.* **2016**, *107*, 282–290. [CrossRef]
19. Nayeem, N.; Sauma, S.; Ahad, A.; Rameau, R.; Kebadze, S.; Bazett, M.; Park, B.J.; Casaccia, P.; Prabha, S.; Hubbard, K.; et al. Insights into Mechanisms and Promising Triple Negative Breast Cancer Therapeutic Potential for a Water-Soluble Ruthenium Compound. *ACS Pharmacol. Transl. Sci.* **2024**, *7*, 1364–1376. [CrossRef]
20. Mello-andrade, F.; Guedes, A.P.M.; Pires, W.C.; Velozo-s, V.S.; Delmond, K.A.; Mendes, D.; Molina, M.S.; Matuda, L.; Montes de Sousa, M.A.; Melo-Reis, P.; et al. Ru(II)/amino acid complexes inhibit the progression of breast cancer cells through multiple mechanism-induced apoptosis. *J. Inorg. Biochem.* **2022**, *226*, 111625. [CrossRef]
21. Grozav, A.; Balacescu, O.; Balacescu, L.; Cheminel, T.; Berindan-Neagoe, I.; Therrien, B. Synthesis, Anticancer Activity, and Genome Profiling of Thiazolo Arene Ruthenium Complexes. *J. Med. Chem.* **2015**, *58*, 8475–8490. [CrossRef] [PubMed]
22. Grozav, A.; Miclaus, V.; Vostinaru, O.; Ghibu, S.; Berce, C.; Rotar, I.; Mogosan, C.; Therrien, B.; Loghin, F.; Popa, D.-S. Acute toxicity evaluation of a thiazolo arene ruthenium(II) complex in rats. *Regul. Toxicol. Pharmacol.* **2016**, *80*, 233–240. [CrossRef] [PubMed]

23. Ignat, A.; Lovasz, T.; Vasilescu, M.; Fischer-fodor, E.; Tatomir, C.B.; Cristea, C.; Silaghi-Dumitrescu, L.; Zaharia, V. Heterocycles 27. Microwave Assisted Synthesis and Antitumour Activity of Novel Phenothiazinyl-Thiazolyl-Hydrazine Derivatives. *Arch. Pharm. Chem. Life Sci.* **2012**, *345*, 574–583. [CrossRef] [PubMed]

24. Patra, M.; Joshi, T.; Pierroz, V.; Ingram, K.; Kaiser, M.; Ferrari, S.; Spingler, B.; Keiser, J.; Gasser, G. DMSO-Mediated ligand dissociation: Renaissance for Biological Activity of *N*-Heterocyclic-[Ru(η^6-arene)Cl$_2$] Drug Candidates. *Chem. Eur. J.* **2013**, *19*, 14768–14772. [CrossRef] [PubMed]

25. Jensen, L.J.; Kuhn, M.; Stark, M.; Chaffron, S.; Creevey, C.; Muller, J.; Doerks, T.; Julien, P.; Roth, A.; Simonovic, M.; et al. STRING 8—a global view on proteins and their functional interactions in 630 organisms. *Nucleic Acids Res.* **2009**, *37*, D412–D416. [CrossRef]

26. GraphPad Prism Version 6.0 for Windows. GraphPad Software: Boston, MA, USA. Available online: www.graphpad.com (accessed on 1 November 2022).